Oscillatory control of Delta-like1 in cell interactions regulates dynamic gene expression and tissue morphogenesis

Hiromi Shimojo,[1,2] Akihiro Isomura,[1,3] Toshiyuki Ohtsuka,[1,4,5] Hiroshi Kori,[3,6] Hitoshi Miyachi,[1] and Ryoichiro Kageyama[1,2,3,4,5]

[1]Institute for Virus Research, Kyoto University, Shogoin-Kawahara, Sakyo-ku, Kyoto 606-8507, Japan; [2]World Premier International Research Initiative–Institute for Integrated Cell-Material Sciences (WPI-iCeMS), Kyoto University, Kyoto 606-8501, Japan; [3]Japan Science and Technology Agency, Core Research for Evolutional Science and Technology (CREST), Kawaguchi, Saitama 332-0012, Japan; [4]Kyoto University Graduate School of Medicine, Kyoto 606-8501, Japan; [5]Kyoto University Graduate School of Biostudies, Kyoto 606-8501, Japan; [6]Department of Information Sciences, Ochanomizu University, Tokyo 112-8610, Japan

Notch signaling regulates tissue morphogenesis through cell–cell interactions. The Notch effectors Hes1 and Hes7 are expressed in an oscillatory manner and regulate developmental processes such as neurogenesis and somitogenesis, respectively. Expression of the mRNA for the mouse Notch ligand Delta-like1 (Dll1) is also oscillatory. However, the dynamics of Dll1 protein expression are controversial, and their functional significance is unknown. Here, we developed a live-imaging system and found that Dll1 protein expression oscillated in neural progenitors and presomitic mesoderm cells. Notably, when Dll1 expression was accelerated or delayed by shortening or elongating the Dll1 gene, Dll1 oscillations became severely dampened or quenched at intermediate levels, as modeled mathematically. Under this condition, *Hes1* and *Hes7* oscillations were also dampened. In the presomitic mesoderm, steady Dll1 expression led to severe fusion of somites and their derivatives, such as vertebrae and ribs. In the developing brain, steady Dll1 expression inhibited proliferation of neural progenitors and accelerated neurogenesis, whereas optogenetic induction of Dll1 oscillation efficiently maintained neural progenitors. These results indicate that the appropriate timing of Dll1 expression is critical for the oscillatory networks and suggest the functional significance of oscillatory cell–cell interactions in tissue morphogenesis.

[*Keywords*: Dll1; oscillation; neural development; somite segmentation; time-lapse imaging]

Supplemental material is available for this article.

Received August 24, 2015; revised version accepted November 23, 2015.

Cell–cell interactions play an important role in coordinated cell differentiation during tissue morphogenesis. Notch signaling is known to regulate such cell–cell interactions during development (Artavanis-Tsakonas et al. 1999; Fortini 2009; Kopan and Ilagan 2009; Pierfelice et al. 2011). The ligand Delta-like1 (Dll1), expressed on signal-sending cells, activates Notch receptor on neighboring receiving cells, where the transcriptional repressor Hes1 is induced (Jarriault et al. 1995; Ong et al. 2006). Hes1 represses the expression of Dll1, thereby making receiving cells Dll1-negative. Thus, Dll1-positive cells inhibit their neighboring cells from also becoming Dll1-positive, a process known as lateral inhibition. In this way, Notch signaling generates heterogeneous cell populations, forming mixtures of Dll1-positive and Dll1-negative cells in a so-called "salt and pepper pattern." This pattern seems to be dynamic, as it has been shown that Hes1 expression oscillates with a period of ~2–3 h by negative feedback in many cell types (Jouve et al. 2000; Hirata et al. 2002; Shimojo et al. 2008; Imayoshi et al. 2013). In neural progenitors, Hes1 oscillation periodically represses the expression of proneural factors such as Ascl1/Mash1 and Neurog2, thereby inducing their oscillatory expression (Shimojo et al. 2008; Imayoshi et al. 2013). As a result, *Dll1* mRNA expression is also oscillatory because proneural factors activate and Hes1 represses *Dll1* expression periodically (Shimojo et al. 2008), indicating that the salt and pepper pattern of *Dll1* mRNA is not static but represents a snapshot of oscillatory expression (Shimojo et al.

Corresponding authors: rkageyam@virus.kyoto-u.ac.jp, hshimojo@virus.kyoto-u.ac.jp
Article is online at http://www.genesdev.org/cgi/doi/10.1101/gad.270785.115. Freely available online through the *Genes & Development* Open Access option.

2008; Kageyama et al. 2008). However, it remains to be determined whether Dll1 protein expression is also dynamic in neural progenitors.

It has been shown that the expression dynamics of various transcription factors are very important for their activities (Levine et al. 2013; Purvis and Lahav 2013; Isomura and Kageyama 2014). For example, the proneural factor Ascl1 has opposing functions depending on its expression patterns (Castro et al. 2011): When Hes1 expression oscillates, Ascl1 is also expressed in an oscillatory manner and activates proliferation of neural progenitors, whereas when Hes1 expression disappears, Ascl1 is expressed in a sustained manner and induces cell cycle exit and neuronal differentiation (Imayoshi et al. 2013; Imayoshi and Kageyama 2014). These data indicate that oscillatory versus sustained expression dynamics are very important for the activities of some transcription factors. However, even if Dll1 protein expression oscillates in neural progenitors, it remains to be analyzed whether Dll1 oscillations play any role in neural development.

Dll1-mediated cell–cell interactions also play an important role in somitogenesis, during which a bilateral pair of somites are periodically segmented from the anterior part of the presomitic mesoderm (PSM) (Hrabe de Angelis et al. 1997; Pourquié 2011). In the mouse PSM, expression of the Notch effector gene *Hes7* oscillates in synchrony in neighboring cells, and those cells that express Hes7 in phase in the anterior PSM form the same somite (Bessho et al. 2001). This synchronized oscillation critically depends on the Notch signaling modulator Lunatic fringe (Lfng); without Lfng, Hes7 oscillation becomes out of synchrony, resulting in severe segmentation defects (Evrard et al. 1998; Zhang and Gridley 1998; Niwa et al. 2011). During this process, *Dll1* mRNA expression oscillates in the PSM (Maruhashi et al. 2005), but the expression dynamics of mouse Dll1 protein are rather controversial; conflicting results have been reported showing that Dll1 protein expression in the mouse PSM is both dynamic and static (Okubo et al. 2012; Bone et al. 2014). Thus, the dynamics of Dll1 protein expression in the PSM also remain to be clarified. Furthermore, it was previously reported that somite segmentation proceeds under steady activation of Notch signaling, forming up to 18 segmented somites (Feller et al. 2008), and thus, even if Dll1 protein expression oscillates, whether this dynamic expression has any role in the segmentation clock remains to be analyzed.

To resolve these issues, we first developed a time-lapse imaging system to monitor Dll1 protein expression and showed that Dll1 protein expression is oscillatory in PSM cells and neural progenitors. We next generated mutant mice in which Dll1 expression was accelerated or delayed, resulting in it being mostly steady or nonoscillatory, a phenomenon known as "amplitude death" or "oscillation death" of coupled oscillators in mathematical modeling (Ramana Reddy et al. 1998). By using these mutant mice, we examined how neural development and somite segmentation are affected by steady Dll1 expression to understand the functional significance of Dll1 oscillation in tissue morphogenesis.

Results

Generation of knock-in mice for time-lapse imaging of Dll1 protein expression

To monitor Dll1 protein expression by live imaging, we inserted luciferase cDNA into the Dll1 gene so that the Dll1-luciferase fusion protein is expressed from the endogenous locus. The firefly (Fluc), emerald (Eluc), or red (Rluc) luciferase cDNA was knocked in at the last exon of the Dll1 gene in mouse embryonic stem (ES) cells (Supplemental Fig. S1A). Each luciferase cDNA was fused in-frame with the 3′ end of the *Dll1*-coding region. Homologous recombinant ES cells were used to generate chimeric mice, which were then crossed with mice ubiquitously expressing flippase to remove the neo gene (Supplemental Fig. S1A). Heterozygous mice derived from each knock-in ES line were born normally. However, homozygous Dll1-Eluc knock-in mice (DE/DE) showed segmentation defects (Supplemental Fig. S1C, right) and were not born, suggesting that the Dll1-Eluc fusion protein is nonfunctional. In contrast, homozygous Dll1-Fluc knock-in (DL/DL) and Dll1-Rluc knock-in (DR/DR) mice developed normally without apparent segmentation defects (Supplemental Fig. S1B,D, right) and were born. Analysis of skeletal preparations of neonates indicated that homozygous Dll1-Fluc knock-in mice had slight segmentation defects in the tail region but no apparent abnormality in the body vertebrae or ribs (Supplemental Fig. S1E, right), while homozygous Dll1-Rluc knock-in mice had no apparent abnormalities (Supplemental Fig. S1F, right). These results suggest that the Dll1-Fluc fusion protein is slightly hypomorphic but functions almost normally, while the Dll1-Rluc fusion protein is fully functional. Because Dll1-Fluc is much brighter than Dll1-Rluc, we decided to use both lines for live imaging and obtained the same results. In both lines, snapshot images of the luciferase reporter expression were very similar to the immunostaining for Dll1 in both neural progenitors and the PSM (Supplemental Fig. S1G,H). We also found that both wild-type Dll1 and Dll1-Fluc fusion proteins have similar half-lives, ~50 min and ~52.5 min, respectively (Supplemental Fig. S1I). These results together suggest that the live luminescence imaging captured the endogenous Dll1 protein expression well.

Dynamic Dll1 protein expression in PSM cells and neural progenitors

We next examined Dll1 expression during somite formation. It has been shown that the expression of many genes, such as that encoding the Notch effector Hes7 or the Notch modulator Lfng, oscillates in the PSM and that each cycle leads to the formation of a pair of somites (Pourquié 2011; Oates et al. 2012). *Dll1* mRNA is also expressed in the PSM, and ablation of *Dll1* leads to severe segmentation defects (Hrabe de Angelis et al. 1997). It was reported that *Dll1* mRNA expression dynamically changes in the PSM (Maruhashi et al. 2005). However, the precise pattern of *Dll1* mRNA expression in the

PSM was not known. Therefore, we used the mice carrying pDll1-Ub-Luc (Fig. 1A), a ubiquitinated luciferase reporter under the control of the *Dll1* promoter and enhancer, which monitors the production of *Dll1* mRNA (Shimojo et al. 2008), to examine how *Dll1* mRNA expression changes in the PSM. Caudal parts of embryonic day 10.5 (E10.5) embryos containing the PSM were cultured with luciferin, and bioluminescence images were examined. Time-lapse imaging analysis showed that *Dll1* mRNA expression changed dynamically throughout the PSM while being lower in the caudal region and higher in the rostral region, on average (Fig. 1B,C; Supplemental Movie S1). Spatiotemporal analysis revealed that *Dll1* mRNA expression clearly oscillated in the PSM, propagating rostrally and reaching S−1, a region just caudal to the next forming somite, S0 (Fig. 1C–E). We next used E10.5 Dll1-Rluc knock-in mice for time-lapse imaging analysis of Dll1 protein expression (Fig. 1F). Dll1 protein expression was observed in the PSM (Fig. 1G; Supplemental Movie S2). The oscillatory expression was somewhat difficult to observe because of low amplitudes, but spatiotemporal profiling clearly revealed that Dll1 protein expression oscillated and propagated rostrally in the PSM (Fig. 1H–J). The Dll1 protein expression domain in S−1 regressed caudally in a stepwise manner of one somite length during segmentation, when S−1 became the new S0, while a wave of Dll1 protein expression progressed rostrally, reaching the new S−1 (Fig. 1I). The oscillatory expression was more evident when the rate of change (temporal difference) in Dll1 protein expression was

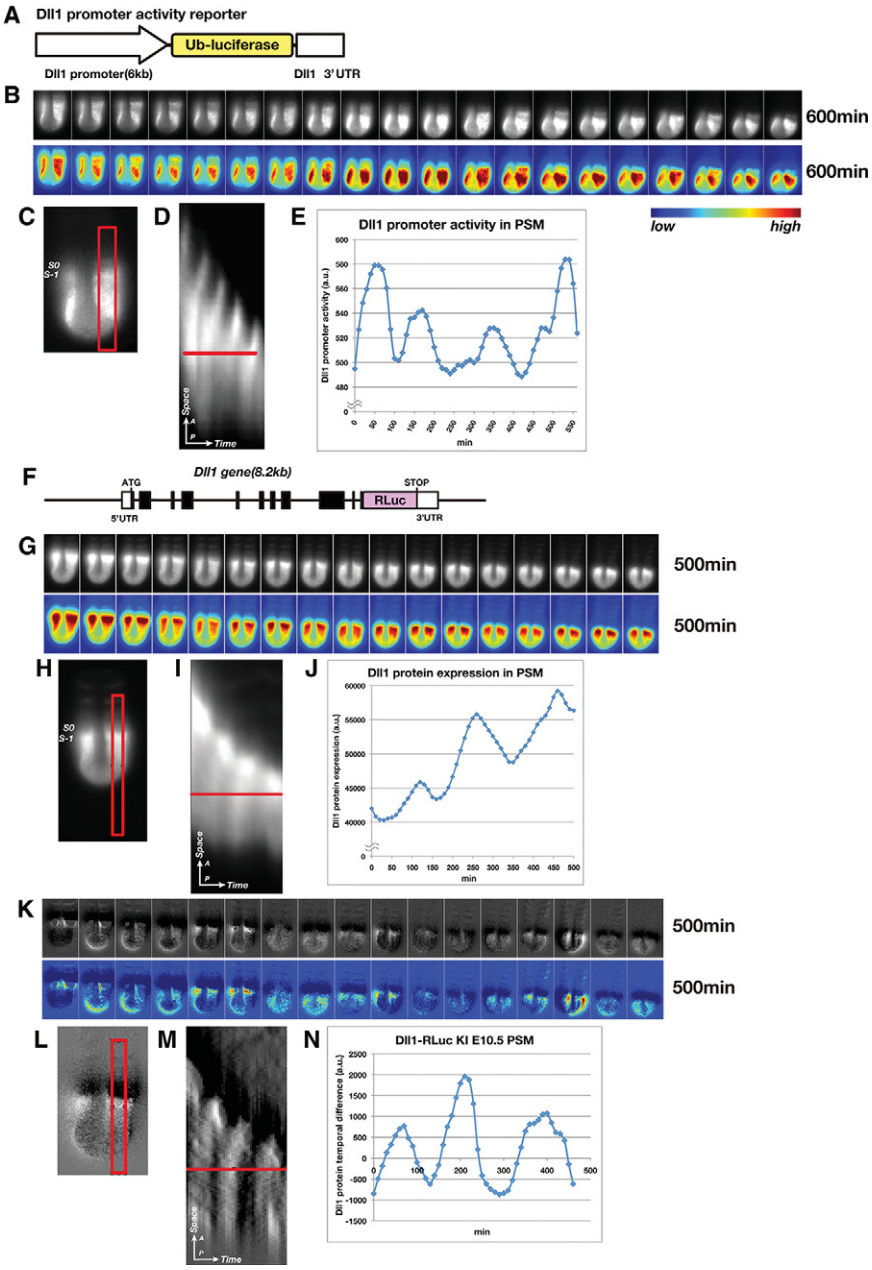

Figure 1. Time-lapse imaging analysis of Dll1 expression in the PSM. (*A*) Structure of the *Dll1* promoter reporter pDll1-Ub-Fluc, which monitors *Dll1* mRNA expression. (*B*) Time-lapse imaging of *Dll1* mRNA expression in the PSM at E10.5. (*Bottom* panels) The signal intensity is also shown by pseudocolors. (*C*) Bioluminescence image of the PSM in a pDll1-Ub-Fluc transgenic mouse. (*D*) Spatiotemporal profile of *Dll1* mRNA expression obtained from *B*. (*E*) Quantification of *Dll1* mRNA expression in the PSM. *Dll1* mRNA expression was quantified along the red line in *D*. (*F*) Structure of the Dll1 protein reporter (Dll1-Rluc knock-in [KI] mice). Rluc cDNA was inserted in-frame into the 3′ end of the *Dll1*-coding region. (*G*) Time-lapse imaging of Dll1 protein expression in the PSM of a Dll1-Rluc knock-in mouse at E10.5. (*Bottom* panels) The signal intensity is also shown by pseudocolors. (*H*) Bioluminescence image of the PSM of a Dll1-Rluc knock-in mouse. (*I*) Spatiotemporal profile of Dll1 protein expression obtained from *G*. (*J*) Quantification of Dll1 protein expression in the PSM. Dll1 protein expression was quantified along the red line in *I*. (*K*) Temporal differences in the rate of change in Dll1 protein expression in the PSM of a Dll1-Rluc knock-in mouse. (*Bottom* panels) The signal intensity is also shown by pseudocolors. (*L*) Bioluminescence image of temporal differences in the rate of change in Dll1 protein expression in the PSM of a Dll1-Rluc knock-in mouse at E10.5. (*M*) Spatiotemporal profile of temporal differences in the rate of change in Dll1 protein expression obtained from *K*. (*N*) Quantification of temporal differences in the rate of change in Dll1 protein expression along the red line in *M*.

extracted. This analysis clearly showed that Dll1 protein expression was activated in the caudal region and propagated rostrally, reaching S−1 (Fig. 1K–N). Furthermore, similar expression patterns were observed in Dll1-Fluc and Dll1-Eluc knock-in mice (Supplemental Fig. S2). The average period of Dll1 protein oscillation in the PSM was 147 min ± 8.6 min. This wave propagation pattern of Dll1 oscillation indicated that Dll1 expression oscillates in phase in neighboring PSM cells but that the oscillation phase is delayed rostrally.

To elucidate the *Dll1* mRNA expression dynamics in neural progenitors, we examined the neural tube of E10.5 transgenic mice carrying pDll1-Ub-Luc. *Dll1* mRNA expression oscillated dynamically in the developing nervous system (Fig. 2A–C; Supplemental Movie S3). Cultured neural progenitors carrying the same reporter also exhibited oscillatory expression that appeared to be anti-phase or out of phase in neighboring cells, in contrast to PSM cells (Fig. 2D,F; Supplemental Fig. S3; Supplemental Movie S4). We then examined Dll1 protein expression in E10.5 Dll1-Fluc and Dll1-Rluc knock-in mice to determine whether it is also dynamic in neural progenitors. Quantification analysis of time-lapse imaging indicated that Dll1 protein expression did oscillate in these cells (Fig. 2E,G; Supplemental Movie S5; Supplemental Fig. S3). The average period of Dll1 protein oscillation in neural progenitors was 143 min ± 4.6 min. In many dividing neural progenitors, the protein was distributed into both daughter cells, but Dll1 expression soon started to oscillate in an anti-phase or out-of-phase manner between two daughter cells, which most likely remained neural progenitors (Fig. 2E,G). Similar results were observed in neural progenitors transfected with the Dll1-Fluc reporter under the control of the 6-kb *Dll1* promoter (Supplemental Fig. S4).

Taken together, these results indicated that Dll1 expression oscillates dynamically in both PSM cells and neural progenitors in in-phase and out-of-phase manners, respectively, at not only the mRNA level but also the protein level.

Generation of Dll1 *type 1 and type 2 mutant mice*

To examine the significance of Dll1 oscillation in embryogenesis, we generated transgenic mice that expressed Dll1 at steady levels under the control of the *mesogenin1* and *nestin* promoters, which induce gene expression in the PSM and neural progenitors, respectively. These mice exhibited defects in both vertebral formation and neural development (data not shown). However, because their Dll1 expression levels were much higher than those in wild-type mice, it is possible that the defects were caused by the high levels rather than its steady expression.

To overcome this issue, we next employed an alternative approach. We showed previously that deleting introns from *Hes7* accelerated the expression by 5–19 min, leading to dampened oscillation (Takashima et al. 2011; Harima et al. 2013). We therefore attempted to accelerate *Dll1* expression by deleting its introns. The intronic delay of expression of *Dll1*, which has 10 introns, was measured using two luciferase reporters: one containing all *Dll1* exon and intron sequences (pUAS-Dll1 wild-type reporter) and the other containing only *Dll1* exon sequences (pUAS-Dll1 type 1 mutant reporter) (Supplemental Fig. S5A). Both reporters were placed under the control of the UAS promoter and the light-switchable transcriptional activator pPGK-hGAVPO (Wang et al. 2012; Imayoshi et al. 2013). Blue light illumination activated hGAVPO, which induced the expression under the control of the UAS promoter, and the induction of the luciferase activity was compared between the two reporters. As expected, the reporter expression was accelerated when introns were removed: The expression occurred ~6 min faster with the Dll1 type 1 mutant reporter (Supplemental Fig. S5B,C, blue line) than with the Dll1 wild-type reporter (Supplemental Fig. S5B,C, green line). Because 5-min acceleration of Hes7 expression led to dampened oscillation, we decided to generate *Dll1* intronless mice (*Dll1* type 1 mutant mice). We next examined the expression from a longer Dll1 gene, which would delay its expression. We thus generated another reporter carrying all exon and intron sequences with insertion of Dll1-Fluc cDNA into the first exon (pUAS-Dll1 type 2 mutant reporter) and examined how the timing of the reporter expression was affected. The reporter expression (Supplemental Fig. S5B,C, red line) was delayed by ~6 min compared with the Dll1 wild-type reporter. Because this delay should also affect oscillatory expression, we decided to generate these mutant mice as well (*Dll1* type 2 mutant mice).

For generation of *Dll1* type 1 mutant mice, a targeting vector containing the intronless Dll1 gene with the Fluc cDNA fused in-frame at the 3′ end was used (Supplemental Fig. S5D). Fluc cDNA was inserted to monitor Dll1 protein expression in the mutant background because the Dll1-Fluc fusion protein functioned normally during neurogenesis and somitogenesis except for the tail region (Supplemental Fig. S1B,E). For generation of *Dll1* type 2 mutant mice, Dll1-Fluc cDNA was knocked in into the first exon of *Dll1* (Supplemental Fig. S5E). Each targeting vector was introduced into mouse ES cells, and homologous recombinants were obtained. These recombinant ES cells were used to make chimeric mice, which were then crossed with mice ubiquitously expressing flippase to remove the neo gene (Supplemental Fig. S5D,E). Heterozygous mutant mice derived from the recombinant ES cells were born normally, and, from these mice, we generated homozygous mice (*Dll1* type 1 and type 2 mutant mice). Both types of homozygous *Dll1* mutant mice were mostly lethal (no homozygote survived postnatally among ~50 pups for type 1 and ~20 pups for type 2). We therefore examined these mutant embryos and obtained very similar phenotypes, as described below.

Steady Dll1 expression in the PSM led to segmentation defects

Immunostaining with Dll1 antibody showed that Dll1 protein expression levels in the PSM of both types of *Dll1* mutant mice were similar to those in wild-type mice, suggesting that Dll1 levels were not significantly

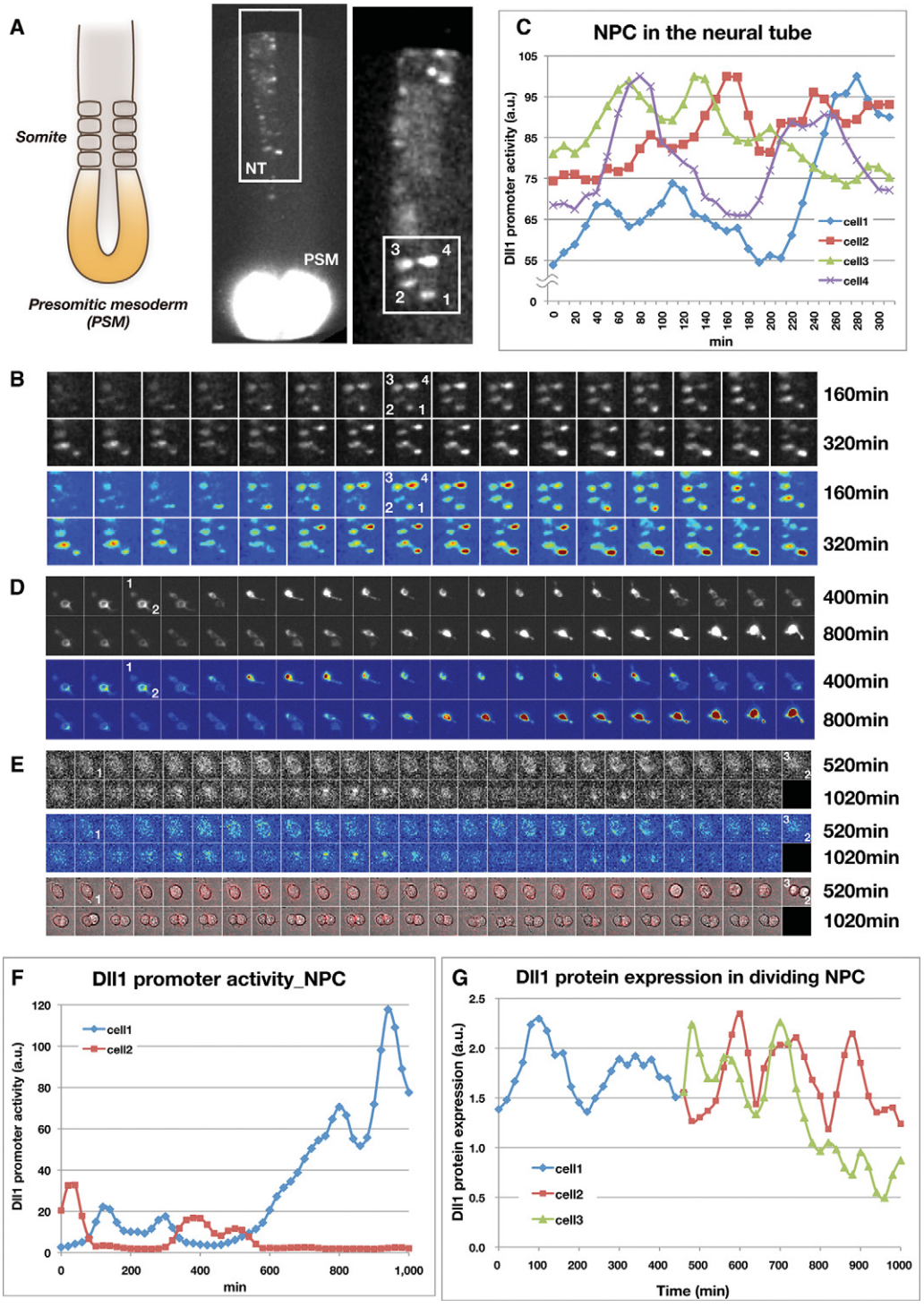

Figure 2. Time-lapse imaging analysis of Dll1 expression in neural progenitors. (*A*, *left*) Illustration of the caudal part of a mouse embryo. (*Middle*) Bioluminescence image of the caudal part of a pDll1-Ub-Fluc transgenic mouse at E10.5. (NT) Neural tube. (*Right*) Enlarged image of the neural tube of a pDll1-Ub-Fluc transgenic mouse. (*B*) Time-lapse imaging of *Dll1* mRNA expression in neural progenitors prepared from a pDll1-Ub-Fluc transgenic mouse. Time-lapse images of numbered cells in *A* are shown. (*C*) Quantification of *Dll1* mRNA expression in each of four neural progenitors obtained from time-lapse imaging. The cell-identifying numbers correspond to those in *A* (*right* panel) and *B*. (*D*) Time-lapse imaging of *Dll1* mRNA expression in cultured neural progenitors carrying the pDll1-Ub-Fluc reporter. (*E*) Time-lapse imaging of Dll1 protein expression in neural progenitors prepared from a Dll1-Fluc knock-in mouse. Pseudocolor and phase-contrast images are also shown. (*F*) Quantification of *Dll1* promoter activities in each of two neural progenitors in *D*. (*G*) Quantification of Dll1 protein expression in neural progenitors in *E*.

affected in these mutant mice (Fig. 3A,B). A longer *Dll1* mRNA was expressed in *Dll1* type 2 mutant mice, as expected (Supplemental Fig. S6). We next performed time-lapse imaging analysis of Dll1 protein expression in explant cultures of the PSM at E10.5. Spatiotemporal expression analysis showed that Dll1 protein expression was rather static in both types of *Dll1* mutant mice, exhibiting only very small oscillation amplitudes or no clear oscillatory changes (Fig. 3D; Supplemental Fig. S7A–E; Supplemental Movie S6), in contrast to the heterozygous mice, which exhibited normal oscillatory expression of Dll1 protein (Fig. 3C). Analysis of the rate of change in Dll1 protein expression showed that there was no clear oscillatory activation after the first nonspecific one (Fig. 3F,H; Supplemental Fig. S7F–I; Supplemental Movie S6), in contrast to that in the heterozygous mice, which showed periodic activation of Dll1 protein expression over time during culture (Fig. 3E,G; Supplemental Movie S6). These data indicated that oscillatory expression of Dll1 protein in the PSM became severely dampened or nonoscillatory at intermediate levels in both types of *Dll1* mutant mice, suggesting that accelerated or delayed Dll1 expression leads to smaller amplitudes or quenching of coupled Dll1 oscillations.

We next examined whether somitogenesis is affected by rather steady Dll1 expression in the PSM. In wild-type and heterozygous mice, *Uncx4.1* expression was localized to the caudal half of each somite (Fig. 4K,L,N), whereas in both types of homozygous *Dll1* mutant embryos, somites were severely fused, resulting in disorganized and diffuse *Uncx4.1* expression (Fig. 4M,O). Furthermore, in wild-type and heterozygous controls, vertebrae and ribs were clearly segmented (Fig. 4P,Q,T,U), whereas their segmentation was defective in both types of homozygous *Dll1* mutant mice at E14.5 (Fig. 4R,S,V,W), indicating that somite formation was disorganized by steady Dll1 expression.

To understand the mechanism of the segmentation defects, we examined the expression of genes involved in somite formation. Hes7 is an essential oscillating factor that regulates somite segmentation (Bessho et al. 2001; Sparrow et al. 2012). Wild-type and heterozygous mutant embryos displayed various patterns of *Hes7* expression in the PSM, indicating that *Hes7* expression oscillates (Fig. 4A,B,D). In contrast, in the PSM of both types of homozygous *Dll1* mutant mice, *Hes7* expression did not show various patterns but occurred almost uniformly (Fig. 4C,E), suggesting that *Hes7* oscillation was severely dampened or abolished. Similarly, *Lfng* expression, which also oscillates under the control of Hes7 oscillation, displayed various patterns in the wild-type and heterozygous mutant PSM (Fig. 4F,G,I). However, *Lfng* expression was downregulated and did not show various patterns in the homozygous mutant PSM (Fig. 4H,J), probably due to steady Hes7 expression because Hes7 represses *Lfng* expression (Bessho et al. 2003). It has been shown that both steady expression of *Hes7* and loss of *Lfng* expression lead to somite fusion (Evrard et al. 1998; Zhang and Gridley 1998; Takashima et al. 2011). These results suggest that the severely reduced amplitudes or quenching of coupled Dll1 oscillators dampens the dynamic expression of *Hes7* and *Lfng*, thereby leading to defects in somite segmentation.

Steady Dll1 expression in neural progenitors led to defects of neural development

We further examined the developing nervous system of both types of *Dll1* mutant mice. In situ hybridization analysis showed that *Dll1* expression in the developing nervous systems of both types of homozygous mutants was similar to that in wild-type and heterozygous mutant mice (Fig. 5A; Supplemental Fig. S8A–C,E). While *Dll1* mRNA expression exhibited a 1.6-fold increase in type 2 mutant neural progenitors compared with the wild type (Supplemental Fig. S8E), this increase was within a normal range of *Dll1* mRNA oscillation. However, time-lapse imaging of Dll1 protein expression in neural progenitors of these mutant mice showed it to be rather static (Fig. 5B–E), in contrast to oscillatory expression in the wild type (Fig. 2G). These data indicated that oscillatory expression of Dll1 protein in neural progenitors also became severely dampened or nonoscillatory at intermediate levels in these mutant mice, suggesting that accelerated or delayed Dll1 expression leads to smaller amplitudes or amplitude/oscillation death of coupled Dll1 oscillators.

We next examined the effects of steady Dll1 expression on Notch signaling in neural progenitors. Dll1-induced activation of Notch signaling leads to processing of Notch protein, releasing the Notch intracellular domain (NICD). The NICD was expressed in the ventricular zone of both types of *Dll1* mutant mice at levels similar to the wild type, although variations in the expression levels were smaller in the mutants (Fig. 6A–D; Supplemental Fig. S8F,I). In addition, the Notch effectors Hes1 and Hes5, whose expression depends on NICD, were expressed in the ventricular zone of both types of *Dll1* mutant mice at levels similar to the wild type (Fig. 6E–J; Supplemental Fig. S8A–D,G,J). These results suggested that Notch signaling was active in the mutants, as it was in the wild type. Although variations of Hes1 expression levels were larger in both mutants than in the wild type (Supplemental Fig. S8J), those in neighboring cells tended to be smaller in the mutants (Supplemental Fig. S8G). Furthermore, time-lapse imaging analysis using the *Hes1* reporter (Fig. 6K) showed that *Hes1* expression was mostly nonoscillatory in both types of mutants (Fig. 6M,N), whereas it oscillated dynamically in wild-type neural progenitors (Fig. 6L), as previously described (Shimojo et al. 2008). Thus, steady Dll1 expression was still able to activate Notch signaling but severely dampened *Hes1* oscillation.

We next examined the effects of steady Dll1 expression on neural development. Expression of the proneural genes *Ascl1* and *Neurog2* was not significantly affected (Fig. 7A,B), although variations in the expression levels in neighboring cells tended to be smaller in the mutants than in the wild type (Supplemental Fig. S8H,K), suggesting that the expression was less dynamic in the mutants. *Neurod1*-expressing post-mitotic neuronal layers were thicker in both types of *Dll1* mutant mice than in wild-type mice (Fig. 7C,D; Supplemental Fig. S9F). Furthermore,

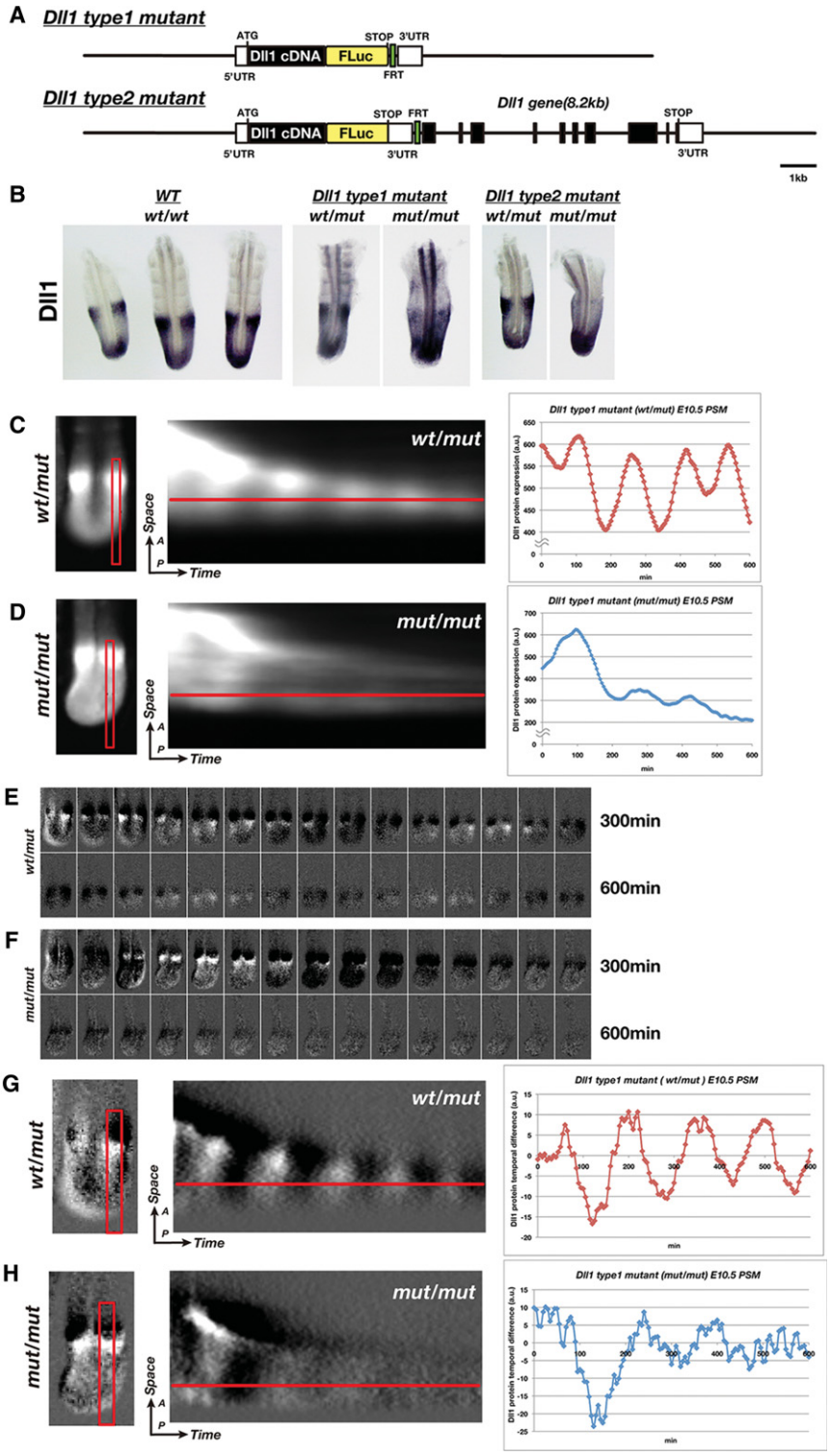

Figure 3. Dll1 expression in the PSM of *Dll1* type 1 and type 2 mutant mice. (*A*) Structures of *Dll1* type 1 and type 2 mutant mouse genes. (*B*) Immunostaining for Dll1 protein in the PSM of both types of heterozygous and homozygous *Dll1* mutant mice as well as the wild type (WT) at E10.5. (*C*, *D*) Analysis of the expression dynamics of Dll1 protein in the PSM of heterozygous (*C*) and homozygous (*D*) *Dll1* type 1 mutant mice at E10.5. (*Left*) Bioluminescence images of Dll1 protein in the PSM. (*Middle*) Spatiotemporal profiles of Dll1 protein expression in the boxed regions in the *left* panels. (*Right*) Quantification of Dll1 protein expression along the red lines in the *middle* panels. (*E*,*F*) Temporal differences in the rate of change in Dll1 protein expression in the PSM of heterozygous (*E*) and homozygous (*F*) *Dll1* type 1 mutant mice. (*G*, *H*) Analysis of the temporal differences in the rate of change in Dll1 protein expression in the PSM of heterozygous (*G*) and homozygous (*H*) *Dll1* type 1 mutant mice. (*Left*) Extracted images of the temporal difference in the rate of change in Dll1 protein expression in the PSM. (*Middle*) Spatiotemporal profiles of the temporal differences in the rate of change in Dll1 protein expression in the PSM. (*Right*) Quantification of these temporal differences along the red lines shown in the *middle* panels.

expression of the basal progenitor marker Tbr2 and the neuronal marker Tuj1 was increased in both types of *Dll1* mutant mice compared with wild-type mice (Fig. 7E–H), suggesting that the numbers of intermediate progenitors and neurons were increased in these mutant mice. The total volumes of the *Hes5*$^{+}$ ventricular zone were reduced in size in the mutants compared with the wild type (Fig. 7O,P; Supplemental Fig. S9 [cf. A and B], D,E), and the brains of these mutants were 20%–30% smaller than those of wild-type mice (Fig. 7N; Supplemental Fig. S9G,H). Furthermore, the total number of mitotic cells that were positive for phospho-histone H3 was reduced in both types of mutants compared with the wild type (Fig. 7I–K,M). Mitotic cells in the apical region (the

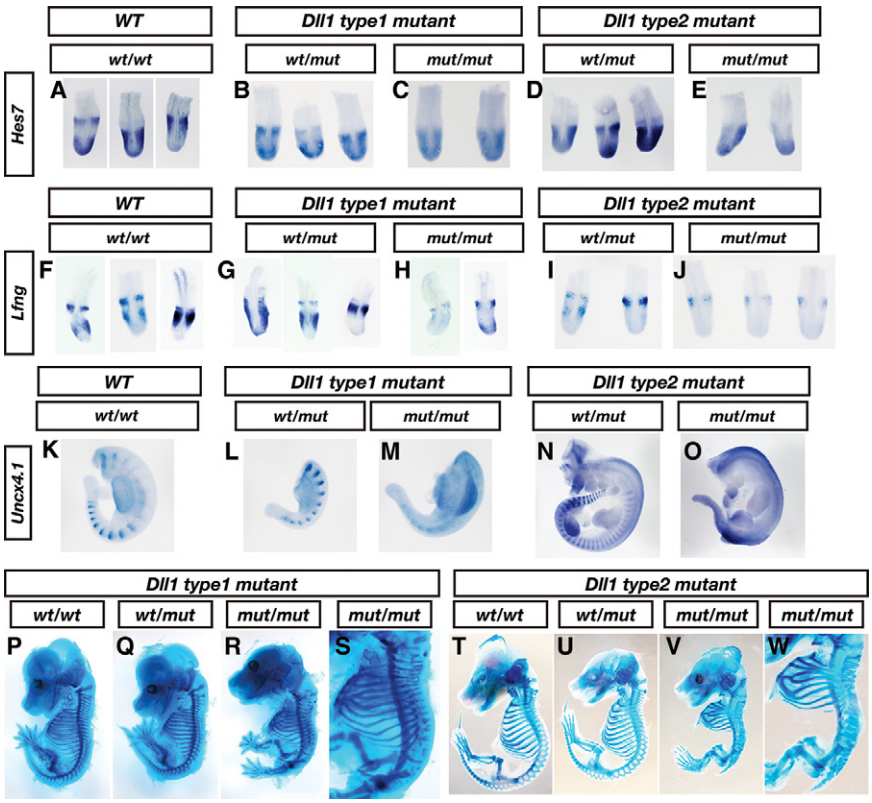

Figure 4. Analysis of somitogenesis and bone structures of *Dll1* type 1 and type 2 mutant mice. (*A–E*) In situ hybridization of *Hes7* in the PSM of wild-type (WT) (*A*, $n = 20$) and heterozygous and homozygous *Dll1* type 1 (*B*, $n = 13$; *C*, $n = 5$) and type 2 (*D*, $n = 6$; *E*, $n = 3$) mutant mice at E10.5. (*F–J*) In situ hybridization of *Lfng* in the PSM of wild-type (*F*, $n = 6$) and heterozygous and homozygous *Dll1* type 1 (*G*, $n = 13$; *H*, $n = 6$) and type 2 (*I*, $n = 6$; *J*, $n = 3$) mutant mice at E10.5. (*K–O*) In situ hybridization of *Uncx4.1* in wild-type (*K*) and heterozygous and homozygous *Dll1* type 1 (*L,M*) and type 2 (*N,O*) mutant mice at E10.5. (*P–W*) Bone staining of wild-type (*P,T*) and heterozygous and homozygous *Dll1* type 1 (*Q–S*) and type 2 (*U–W*) mutant mice at E14.5. *R* and *V* are enlarged in *S* and *W*, respectively.

ventricular side) were reduced in number (Fig. 7I–L), suggesting that neural progenitors underwent premature cell cycle exit when Dll1 expression was steady. However, cell death was not significantly affected in both mutants compared with the wild type (data not shown). Together, these results suggest that the amplitude/oscillation death of coupled Dll1 oscillators severely dampens *Hes1* oscillation and accelerates neuronal differentiation at the expense of mitotic neural progenitors, thereby reducing the size of the brain.

To determine whether Dll1 oscillation favors the maintenance of neural progenitors, we induced oscillatory or sustained Dll1 expression by using the hGAVPO system (Fig. 7Q; Supplemental Fig. S10; Imayoshi et al. 2013). Blue light exposure activated hGAVPO, which induced Dll1-Fluc expression (Fig. 7Q; Supplemental Fig. S10). Light-induced oscillatory expression of Dll1 significantly increased the expression of the progenitor gene *Hes5* (Fig. 7R), whereas light-induced sustained expression upregulated the expression of neuronal genes *Ascl1* and *p21* (Fig. 7S,T). These data suggested that Dll1 oscillation favors maintenance of neural progenitors, whereas sustained Dll1 expression favors neuronal differentiation.

Mathematical modeling of Dll1-mediated intercellular-coupled oscillators for amplitude/oscillation death

We next asked whether the observed phenotypes can be simulated by mathematical modeling, which consists of differential equations (Lewis 2003). It was previously shown that with certain coupling delays, oscillators undergo oscillation quenching, a phenomenon known as "amplitude death" or "oscillation death" in mathematical modeling (Ramana Reddy et al. 1998). In Notch signaling, Hes represses the expression of its own and Dll1 with a delay, while Dll1 activates Hes in a neighboring cell with another delay (Supplemental Fig. S11A, left). These Dll1-Hes oscillators can be simplified as double-negative feedback loops—one with a delay of τ_1 within a cell and the other with a delay of τ_2 from a neighboring cell (Supplemental Fig. S11A, right). Numerical simulations with differential equations suggested that Dll1-Hes oscillators would show in-phase and out-of-phase oscillations depending on different τ_2 values (Supplemental Fig. S11B,C [panels a,c], D). Interestingly, when the τ_2 values for in-phase or out-of-phase oscillation are increased or decreased, coupled oscillations exhibit smaller amplitudes (smaller differences between the maximum and minimum levels) and are eventually quenched with a fixed intermediate value (Supplemental Fig. S11C [panels b,d], D). These results raised the possibility that Dll1-Hes oscillation would undergo "amplitude/oscillation death" when τ_2 was increased or decreased.

It is likely that accelerated or delayed expression of Dll1 would decrease or increase τ_2, the time required for coupling or Dll1–Notch signaling transmission between cells. While precise parameter values in this mathematical modeling remain to be determined, these results suggest that accelerated or delayed Dll1 expression may dampen or quench the oscillator networks, giving the supportive basis for the observed phenotypes in *Dll1* type 1 and type 2 mutant mice (Supplemental Fig. S12).

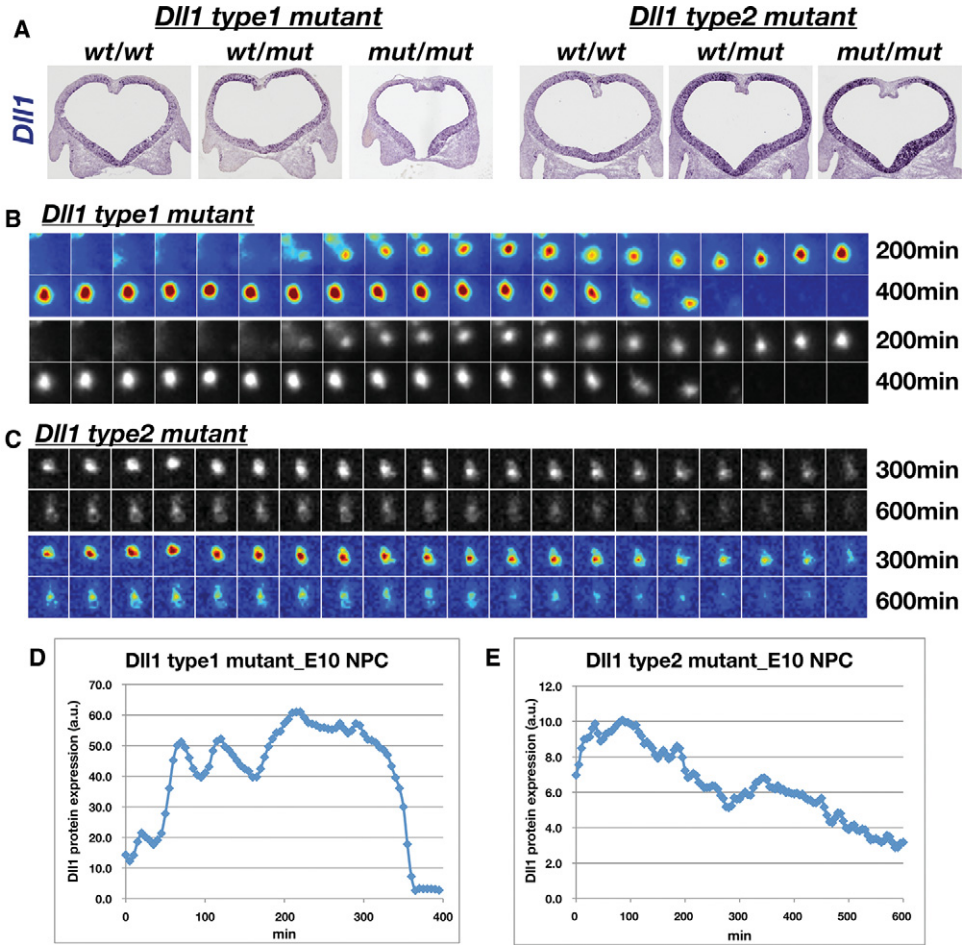

Figure 5. Dll1 expression in neural progenitors of *Dll1* type 1 and type 2 mutant mice. (*A*) In situ hybridization of *Dll1* mRNA in the developing brains of wild-type and heterozygous and homozygous *Dll1* type 1 and type 2 mutant mice at E10.5. (*B*,*C*) Time-lapse imaging of Dll1 protein expression in neural progenitors derived from the telencephalon of homozygous *Dll1* type 1 (*B*) and type 2 (*C*) mutant mice at E10.5. (*D*,*E*) Quantification of Dll1 protein expression in neural progenitors of homozygous *Dll1* type 1 (*D*) and type 2 (*E*) mutant mice in *B* and *C*.

Discussion

Dynamic control of Dll1 in cell–cell interactions

The expression dynamics of Dll1 protein is rather controversial, probably because the changes in Dll1 expression levels are small. Time-lapse imaging analysis clearly showed that Dll1 expression oscillates in phase between neighboring PSM cells and out of phase between neighboring neural progenitors, suggesting that Dll1 dynamically controls cell–cell interactions. This dynamic control is indeed very important because rather static or steady Dll1 expression at intermediate levels dampens *Hes1* and *Hes7* oscillations, thereby leading to severe defects of neural development and somite segmentation, respectively. Thus, dynamic control of Dll1 in cell–cell interactions is critical for the oscillatory networks and tissue morphogenesis.

Steady Dll1 expression may be functional for activation of gene expression in neighboring PSM cells because the Notch effector gene *Hes7* was expressed in the PSM of both *Dll1* type 1 and type 2 mutant mice. However, steady Dll1 is definitely nonfunctional as the segmentation clock because *Hes7* and *Lfng* oscillations are dampened, suggesting that the coupled oscillatory control of Dll1 is essential to drive the segmentation clock (Supplemental Fig. S12). In zebrafish, the Dll1 homolog DeltaC is expressed in an oscillatory manner and regulates their segmentation clock (Mara et al. 2007; Soza-Ried et al. 2014). Thus, the functional significance of the oscillatory expression of Notch ligands seems to be evolutionarily conserved among vertebrates such as mammals and zebrafish.

Similarly, steady Dll1 expression may be functional for activation of gene expression in neighboring neural progenitors because NICD, Hes1, and Hes5 were expressed in neural progenitors of both *Dll1* type 1 and type 2 mutant mice. However, steady Dll1 results in accelerated neuronal differentiation and loss of progenitor pools, and these phenotypes are rather similar to those found in *Dll1*-deficient mice, in which premature neuronal differentiation occurs (Hrabe de Angelis et al. 1997; Yun et al. 2002; Kawaguchi et al. 2008). Thus, steady Dll1 is not functional for proper timing of neuronal differentiation and maintenance

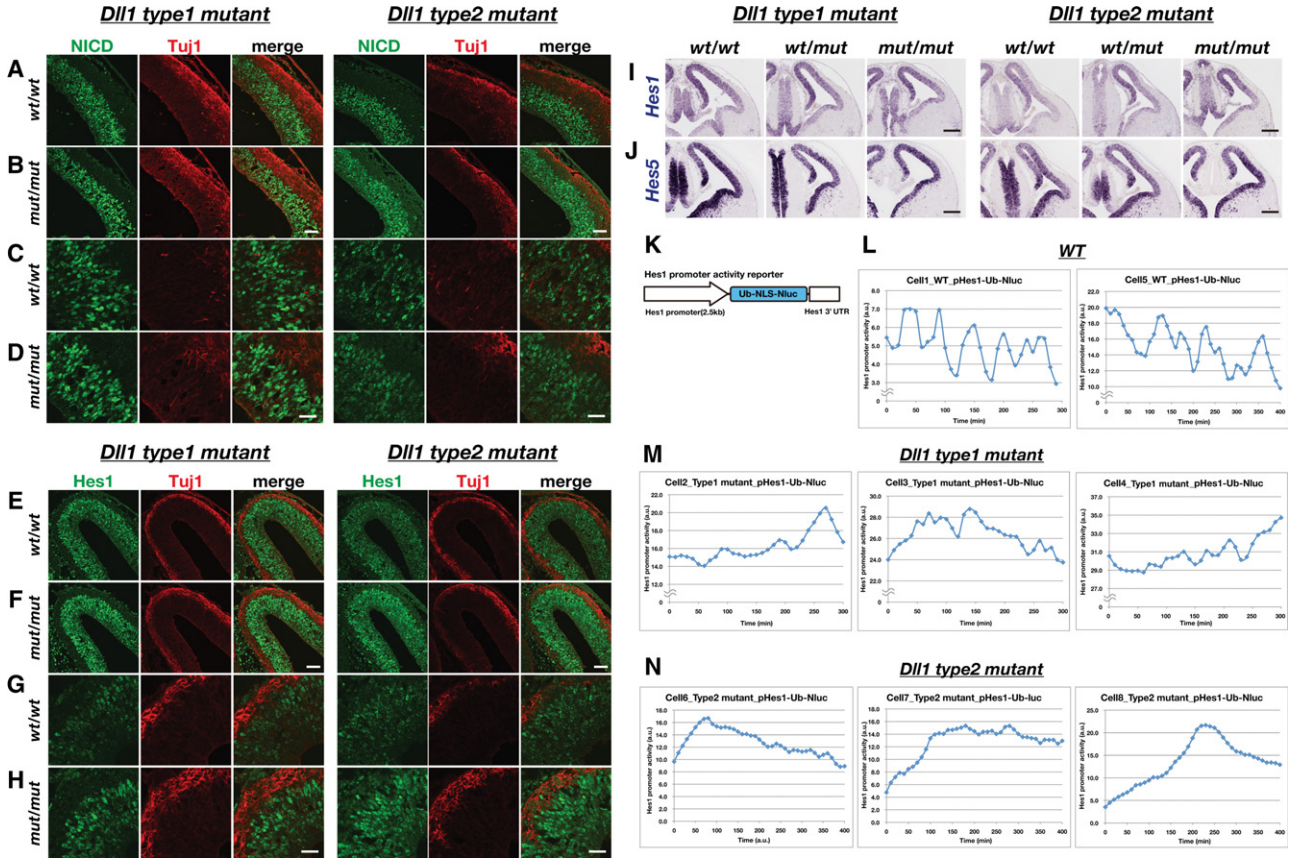

Figure 6. Analysis of Notch signaling genes in *Dll1* type 1 and type 2 mutant mice. (*A–D*) Immunohistochemistry of NICD (green) and Tuj1 (red) in the cortex of wild-type (WT) (*A*,*C*) and homozygous mutant (*B*,*D*) mice at E12.5. (*E–H*) Immunohistochemistry of Hes1 (green) and Tuj1 (red) in the cortex of wild-type (*E*,*G*) and homozygous mutant (*F*,*H*) mice at E12.5. (*I*,*J*) In situ hybridization of *Hes1* (*I*) and *Hes5* (*J*) mRNA in the telencephalon of wild-type and heterozygous and homozygous *Dll1* type 1 and type 2 mutant mice at E12.5. (*K*) Structure of the *Hes1* promoter reporter. (*L–N*) Quantification of *Hes1* expression in neural progenitors in cortical slice cultures of wild-type (*L*) and homozygous *Dll1* type 1 (*M*) and type 2 (*N*) mutant mice. Bars: *A*,*B*,*E*,*F*, 50 μm; *C*,*D*,*G*,*H*, 20 μm; *I*,*J* 300 μm.

of neural progenitors, and Dll1 oscillation is definitely required for normal brain development (Supplemental Fig. S12). The exact mechanism by which sustained Dll1 expression accelerates neuronal differentiation remains to be further analyzed. Steady Dll1 expression dampened *Hes1* oscillation, which may inhibit cell cycle progression in neural progenitors because sustained Hes1 expression inhibits proliferation (Baek et al. 2006). Dll1 oscillation between neural progenitors may be important for mutual activation of Notch signaling at early stages because sufficient Dll1-expressing neurons are not born yet (Kageyama et al. 2008; Shimojo et al. 2008). In agreement with this idea, when Dll1 expression was nonoscillatory, the smaller brain sizes were evident in both *Dll1* type 1 and type 2 mutant mice as early as E12.5 (Fig. 7N), indicating that Dll1 oscillation is required for proliferation and maintenance of neural progenitors at early stages.

Appropriate coupling delays are important for the expression dynamics

We found that both accelerated and delayed Dll1 expression dampened its oscillatory expression, suggesting that the appropriate timing of Dll1 expression is important for its expression dynamics. Our mathematical modeling suggests that when the coupling delay is decreased or increased, both in-phase and out-of-phase oscillations would be dampened or quenched (Supplemental Fig. S11C,D), a phenomenon known as "amplitude/oscillation death" (Ramana Reddy et al. 1998). When Dll1 protein expression became steady, both *Hes1* and *Hes7* oscillations were also dampened in neural progenitors and PSM cells, respectively. These results suggest that appropriate delays in Dll1-mediated Notch signaling transmission between cells are essential for dynamic gene expression.

While our mathematical modeling depicted the gene expression dynamics in both types of *Dll1* mutant mice, it definitely needs more validation and adjustment. For example, dampened or quenched oscillations were caused by just a 6-min acceleration or delay of Dll1 expression. Such a short range of time for oscillations can be quantitatively reproduced by carefully choosing parameter values. However, our model still needs more clarification with further examination of the exact parameter values such as Hill coefficients (*m* and *n* in Supplemental Fig. S11B). It was previously shown that elongation of the Dll1 gene

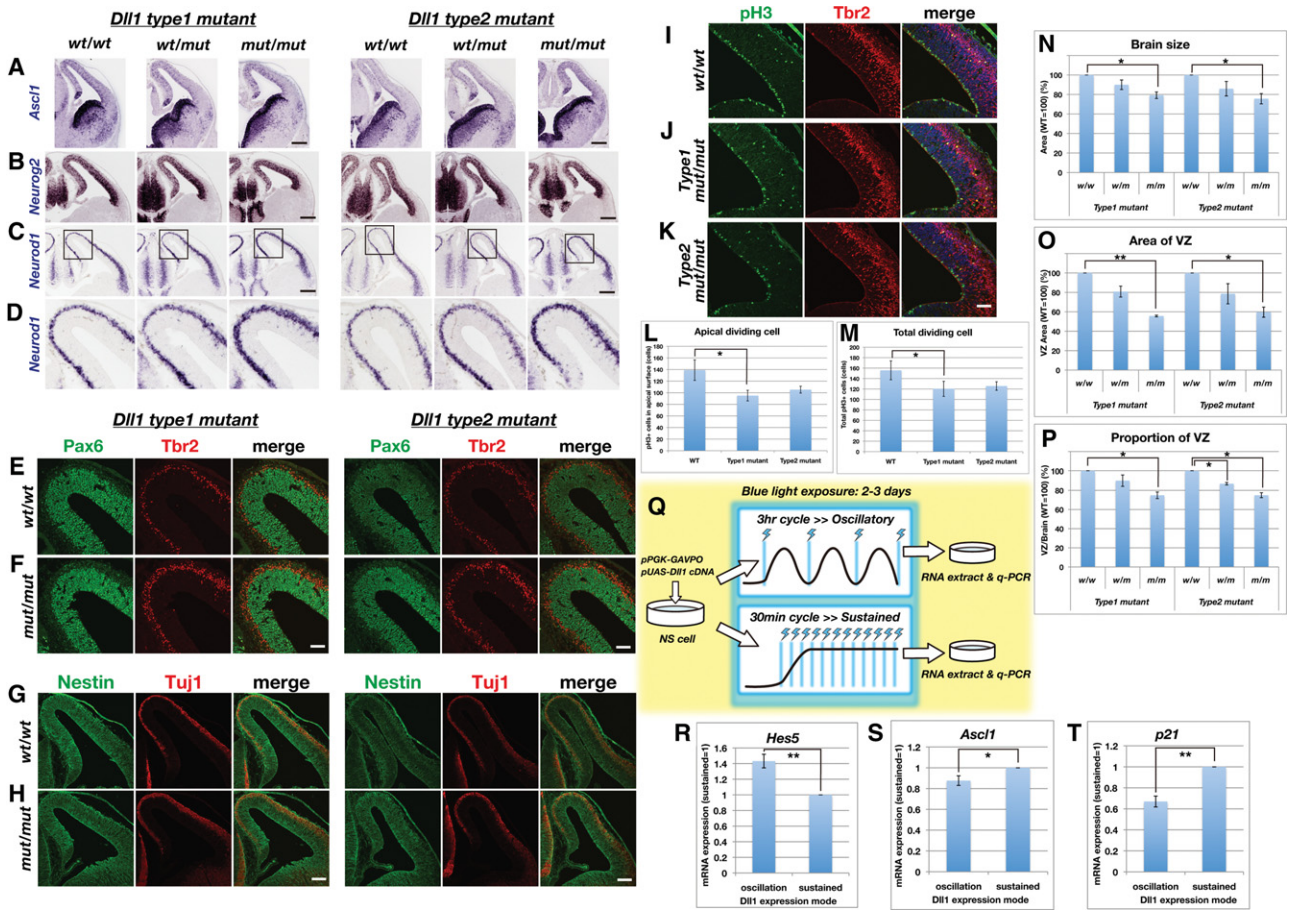

Figure 7. Analysis of neural development in *Dll1* type 1 and type 2 mutant mice. (*A–D*) In situ hybridization of *Ascl1* (*A*), *Neurog2* (*B*), and *Neurod1* (*C*,*D*) in the telencephalons of wild-type (wt/wt) and heterozygous (wt/mut) and homozygous (mut/mut) *Dll1* type 1 and type 2 mutant mice at E12.5. (*E*,*F*) Immunohistochemistry of Pax6 and Tbr2 in the cortices of wild-type (*E*) and homozygous *Dll1* type 1 (*left*) and type 2 (*right*) mutant (*F*) mice at E12.5. (*G*,*H*) Immunohistochemistry of Nestin and Tuj1 in the cortices of wild-type (*G*) and homozygous *Dll1* type 1 (*left*) and type 2 (*right*) mutant (*H*) mice at E12.5. (*I–K*) Immunohistochemistry of phospho-histone H3 (pH3; green) and Tbr2 (red) in the cortices of wild-type (*I*) and homozygous *Dll1* type 1 (*J*) and type 2 (*K*) mutant mice at E12.5. (*L*) The numbers of pH3-positive cells at the apical surface within a 16-μm thickness in wild-type and homozygous *Dll1* type 1 and type 2 mutant cortices at E12.5. (*M*) The numbers of pH3-positive cells within a 16-μm thickness in the wild-type and homozygous *Dll1* type 1 and type 2 mutant cortices at E12.5. (*N*) The brain sizes of heterozygous (w/m) and homozygous (m/m) *Dll1* type 1 and type 2 mutant mice relative to the wild type (w/w) at E10.5–E14.5. (*O*) The areas of the ventricular zones of heterozygous (w/m) and homozygous (m/m) *Dll1* type 1 and type 2 mutant mice relative to the wild type (w/w) at E10.5–E14.5. (*P*) The proportion of the ventricular zones in the telencephalons of wild-type (w/w) and heterozygous (w/m) and homozygous (m/m) *Dll1* type 1 and type 2 mutant mice at E10.5–E14.5. Bars: *A–C*, 300 μm; *E*,*F*, 50 μm; *G*,*H*, 100 μm; *I–K*, 50 μm. (*Q*) Light-induced oscillatory or sustained Dll1 expression by the GAVPO system. Blue light exposure at 3-h and 30-min intervals induced oscillatory and sustained expression, respectively. (*R–T*) The gene expression in neural progenitor cultures was quantified after induction of oscillatory or sustained Dll1 expression. Each value represents the average of at least three independent experiments with error bars. (*) $P < 0.05$; (**) $P < 0.01$, Student *t*-test.

led to segmentation defects but milder phenotypes than our type 2 mutants (Schuster-Gossler et al. 2007). It would be interesting to compare the timing of Dll1 expression in these mutants.

Our modeling also suggests that the coupling delay between neighboring oscillators is different between in-phase and out-of-phase oscillations. However, it is not known whether the delay in Dll1–Notch signaling transmission is different between PSM cells and neural progenitors because of technical difficulty. Previous data suggested that the way of Dll1–Notch signaling transmission seems to be different between these two cell types. Lfng, which is known to modulate Dll1 and Notch activities by glycosylation (Panin et al. 2002), is essential for somitogenesis (Evrard et al. 1998; Zhang and Gridley 1998) but not neurogenesis (Kato et al. 2010). This difference in Lfng requirement may account for different coupling delays in Dll1–Notch signaling transmission between cells. Lfng may also affect the coupling strength of Dll1–Notch interactions between cells, which is another important parameter for gene expression dynamics (Ramana Reddy et al. 1998). Further analysis will be required to establish more complete mathematical modeling.

It was previously shown that introns and their sizes are important for the timing of gene expression (Swinburne et al. 2008; Swinburne and Silver 2008). An artificial genetic network with delayed negative feedback exhibited oscillatory expression; longer introns delayed the timing of gene expression, thereby increasing the periods of oscillatory expression (Swinburne et al. 2008). We previously found that intronic delay is important for Hes7 expression dynamics: Deleting two or all three introns from *Hes7* accelerated its expression by ~5 min and 19 min, respectively, and, in both cases, Hes7 oscillations were severely dampened (Takashima et al. 2011; Harima et al. 2013). In the present study, we found that deleting all introns accelerated the Dll1 expression, while elongating the gene size delayed the Dll1 expression, and both mutations severely dampened or quenched its in-phase and out-of-phase oscillations in neighboring cells. These results suggest that introns and gene sizes are very important for the proper timing and dynamics of Dll1 expression.

Dampened *Hes1* oscillation by steady Dll1 expression was rather unexpected because Hes1 expression autonomously oscillated by negative feedback even in the presence of steady NICD (Imayoshi et al. 2013). When neural progenitors of homozygous *Dll1* mutant mice were dissociated, *Hes1* expression oscillated (data not shown), indicating that *Hes1* oscillation is self-sustaining in individual *Dll1* mutant neural progenitors. Dampened *Hes1* oscillation therefore occurred only when mutant neural progenitors interacted with each other, suggesting that delays in Dll1–Notch signaling transmission regulate oscillatory versus steady gene expression and that Dll1 input at inappropriate times dampens Hes1 oscillation. Thus, the timing of Dll1-mediated cell–cell interactions is very important for expression dynamics of coupled oscillators.

Dynamic control of Notch signaling

It was recently shown that Notch1 protein levels also oscillate in the PSM (Bone et al. 2014). We generated transgenic mice that express Notch1-Fluc fusion proteins under the control of the *Notch1* promoter and enhancer. Our preliminary analysis showed that Notch1 protein levels also changed in both PSM and neural progenitors. However, even at trough phases, Notch1 protein was expressed at relatively high levels, suggesting that Notch1 protein is continuously expressed in these cells (H Shimojo and R Kageyama, unpubl.). Thus, we speculate that Dll1 levels are more important for regulating Dll1–Notch1 signaling transmission, although the exact role of Notch1 expression dynamics remains to be analyzed.

In addition to its dynamic expression, Delta protein undergoes dynamic subcellular translocation and functional modulation (Yamamoto et al. 2010). In *Drosophila*, Delta protein is endocytosed into recycling endosomes to become activated and returns to the plasma membrane. Activated Delta then interacts with Notch of neighboring cells and transendocytoses the Notch extracellular domain, thereby inducing the release of NICD (Parks et al. 2000). Thus, the subcellular localization and the activity of Delta protein are dynamically regulated in *Drosophila* and vertebrates. It is likely that Delta protein on the cell surface is functionally important for intercellular Notch signaling transmission, and further analysis will be required to measure the exact amount of Dll1 protein on the cell surface. This kind of analysis will contribute important information for understanding the mechanisms by which delays in Dll1–Notch signaling transmission are controlled.

Materials and methods

Generation of Dll1-luciferase protein reporter and Dll1-luciferase knock-in mice

All animal experiments were approved by the Institutional Animal Care and Use Committee at Kyoto University. Fluc, Eluc, or Rluc cDNA was inserted in-frame into the 3′ end of the coding region of the Dll1 gene by BAC recombineering. To obtain the Dll1-luciferase protein reporter, the fragments containing the *Dll1* promoter (6 kb), Dll1 gene, luciferase cDNA, and 3′ untranslated region (UTR; 0.7 kb) were retrieved to pBS vector.

Dll1-luciferase knock-in mice were generated for visualization of Dll1 protein expression. A FRT-Neo^R cassette was inserted into the downstream region of luciferase cDNA of each of the BAC constructs described above. The fragment containing from the upstream region (2.5 kb) of the luciferase sequence to the downstream region (8 kb) was retrieved to pMCS-DTA, including diphtheria toxin A-coding sequence. The linearized targeting vector was electroporated into TT2 ES cells, and G418-resistant clones were analyzed by PCR. The homologous recombinant ES cells were injected into eight-cell stage mouse embryos to obtain chimera according to standard procedures. Chimeric mice were crossed with mice ubiquitously expressing FLPe recombinase to delete the neo gene sequence, followed by crossing with wild-type mice to remove FLPe recombinase sequence.

Bioluminescence imaging of the PSM explant culture

Explant culture of the PSM of reporter mice was performed as described previously (Masamizu et al. 2006; Niwa et al. 2011). The tail regions of reporter mice were put on glass-based dishes with 1 mM luciferin (Nacalai Tesque) in 10%FBS/DMEM-F12 medium. The tissue was cultured in 80% O_2 and 5% CO_2 at 37°C. For image analysis, ImageJ software was used as described previously (Niwa et al. 2011). Stack images were applied to spike noise filter to remove signals from cosmic rays and then to Savitzky Golay temporal filter to get clear dynamic expression. For making spatiotemporal profiles, resliced stack images in the anterior–posterior axis were arranged from left to right in the temporal order. The spatiotemporal profiles were applied to plot profiles to obtain the dynamic reporter expression in the temporal order. Temporal difference images of Dll1 expression levels, $\Delta I(x,y; n)$, were obtained by subtracting $I(x,y; n-1)$ from $I(x,y; n)$, where $I(x,y; n)$ is a signal value at the spatial position of (x,y) and the nth frame of the temporal axis.

Bioluminescence imaging of neural progenitor dissociation culture

Neural progenitors at E10.5–E14.5 were dissociated as described previously (Shimojo et al. 2008). They were plated into glass-based dishes with 1 mM luciferin (Nacalai Tesque) in N2/B27 medium (DMEM/F12 supplemented with 1× N2 [Gibco], 1× B27

[Gibco], 1 mM N-acetyl-cysteine, 10 ng/mL bFGF [Invitrogen]). Bioluminescence measurement was performed as previously described (Shimojo et al. 2008).

Bioluminescence imaging of cortical slice cultures

Cortical slice cultures and measurement of bioluminescence were performed as previously described (Shimojo et al. 2008). For the measurement of Hes1 promoter activity, we used ubiquitinated NanoLuc (Ub-Nluc) reporter. Nluc (Promega) is a different type of luciferase, having a small molecular size and using a different type of substrate for generation of bioluminescence. pHes1-Ub-Nluc reporter was introduced into neural progenitors in the cortices of *Dll1* mutant mice at E12.5 by in utero electroporation. Twenty-four hours after electroporation, embryos of *Dll1* mutant mice were harvested, and cortical slices were prepared. For visualization of pHes1-Ub-Nluc reporter, 12 μM EnduRen (Promega) substrate was added to media for detection of Nluc activity.

Generation of Dll1 *mutant knock-in mice*

For generation of *Dll1* type 1 mutant mice, the Dll1 gene regions from ATG to the stop codon were replaced with Dll1 cDNA fused with luciferase cDNA by BAC recombineering. For generation of *Dll1* type 2 mutant mice, the first exon of the Dll1 gene was replaced with Dll1 cDNA fused with luciferase cDNA followed by the 3′ UTR of the Dll1 gene by BAC recombineering. For preparation of the targeting vector of the *Dll1* type 1 mutant, a FRT-Neo^R cassette was inserted into the downstream region of luciferase cDNA. The region from 2.5 kb upstream of the Dll1 cDNA sequence to 8 kb downstream from the FRT-Neo^R cassette was retrieved to the pMCS-DTA vector. In the case of the *Dll1* type 2 mutant, a FRT-Neo^R cassette was inserted into the downstream region of the *Dll1* 3′ UTR following the Dll1 cDNA sequence inserted into the *Dll1* first exon, and the region from 2.5 kb upstream of the Dll1 cDNA sequence to 8 kb downstream from the FRT-Neo^R cassette was retrieved to the pMCS-DTA vector. The linearized targeting vectors were electroporated to TT2 ES cells, and G418-resistant ES clones were analyzed by PCR. The homologous recombinant ES clones were injected into eight-cell stage mouse embryos to obtain chimeric mice. Chimeric mice were crossed with mice ubiquitously expressing FLPe recombinase to delete the neo sequence, followed by crossing with wild-type mice to remove the FLPe recombinase sequence.

In situ hybridization

In situ hybridization was performed as described previously (Bessho et al. 2001; Shimojo et al. 2008).

Bone staining

Bone staining was performed as described previously (Bessho et al. 2001).

Immunohistochemistory

For immunostaining of Hes1, NICD, and Pax6, antigen retrieval was performed in 0.1% Tween20/0.01 M citrate buffer (pH 6.0) using an autoclave (15 min at 105°C). The primary antibodies used were as follows: rabbit anti-Hes1 (Kobayashi et al. 2009) and rabbit anti-NICD (Cell Signaling). Sections were incubated with primary antibodies overnight at 4°C. After being washed in PBS, sections were incubated with secondary antibody (HRP-conjugated anti-rabbit IgG; GE Healthcare) for 90 min at room temperature. After washes in PBS and PBST, color development was enhanced by TSA amplification system (Perkin Elmer) according to the manufacturer's instructions. For immunostaining of Nestin, Tuj1, Pax6, Tbr2, and phosphorylated histone H3 (pH3), sections were incubated with primary antibodies overnight at 4°C. The primary antibodies used were as follows: mouse anti-Nestin (BD Biosciences), rabbit anti-Tuj1 (Covance), mouse anti-Pax6 (DSHB), rabbit anti-Tbr2 (Abcam), and mouse anti-pH3 (Sigma). The secondary antibodies used were as follows: Alexa 594-conjugated anti-rabbit IgG (Molecular Probes) and Alexa 488-conjugated anti-mouse IgG (Molecular Probes). The pH3$^+$ cell numbers and the area sizes were quantified by using every 20 sections (16-μm thickness) of at least three brains of each genotype.

In utero electroporation

In utero electroporation was performed as described previously (Shimojo et al. 2008).

Light-induced Dll1 expression in neural stem cells by the hGAVPO system

Neural stem cells carrying pPGK-hGAVPO and pUAS-Dll1 type 1 mutant reporter were seeded into 24-well dishes and cultured in DMED/F12 supplemented by N2-PLUS reagent, 20 ng/mL bFGF, 20 ng/mL EGF, and 1 mM luciferin. Light-induced Dll1-luciferase expression was monitored by a photonmultiplier with an exposure time of 5 sec at 3-min intervals. Blue light was illuminated every 3 h or every 30 min. Signals were obtained by count per second (cps). After 2–3 d under the blue light stimulation, cells were harvested, and the expression of *Hes5*, *Ascl1*, and *p21* was examined by real-time PCR.

Acknowledgments

We are grateful to Yasutaka Niwa and Fumiko Ogushi for discussion, and Nanae Fujishige for technical help. This work was supported by Core Research for Evolutional Science and Technology (R.K.), Grant-in-Aid for Scientific Research on Innovative Areas (Ministry of Education, Culture, Sports, Science, and Technology, Japan 22123002 [to R.K.] and 24116705 [to H.S.]), Scientific Research (A) (Japan Society for the Promotion of Science 24240049 to R.K.), and Young Scientists (B) (Japan Society for the Promotion of Science 24700354 to H.S.), Takeda Foundation (R.K.), and Platform for Dynamic Approaches to Living System from the Ministry of Education, Culture, Sports, Science, and Technology, Japan.

References

Artavanis-Tsakonas S, Rand MD, Lake RJ. 1999. Notch signaling: cell fate control and signal integration in development. *Science* **284:** 770–776.

Baek JH, Hatakeyama J, Sakamoto S, Ohtsuka T, Kageyama R. 2006. Persistent and high levels of Hes1 expression regulate boundary formation in the developing central nervous system. *Development* **133:** 2467–2476.

Bessho Y, Sakata R, Komatsu S, Shiota K, Yamada S, Kageyama R. 2001. Dynamic expression and essential functions of *Hes7* in somite segmentation. *Genes Dev* **15:** 2642–2647.

Bessho Y, Hirata H, Masamizu Y, Kageyama R. 2003. Periodic repression by the bHLH factor Hes7 is an essential

mechanism for the somite segmentation clock. *Genes Dev* **17:** 1451–1456.

Bone RA, Bailey CSL, Wiedermann G, Ferjentsik Z, Appleton PL, Murray PJ, Maroto M, Dale JK. 2014. Spatiotemporal oscillations of Notch1, Dll1 and NICD are coordinated across the mouse PSM. *Development* **141:** 4806–4816.

Castro DS, Martynoga B, Parras C, Ramesh V, Pacary E, Johnston C, Drechsel D, Lebel-Potter M, Garcia LG, Hunt C, et al. 2011. A novel function of the proneural factor Ascl1 in progenitor proliferation identified by genome-wide characterization of its targets. *Genes Dev* **25:** 930–945.

Evrard YA, Lun Y, Aulehla A, Gan L, Johnson RL. 1998. *lunatic fringe* is an essential mediator of somite segmentation and patterning. *Nature* **394:** 377–381.

Feller J, Schneider A, Schuster-Gossler K, Gossler A. 2008. Noncyclic Notch activity in the presomitic mesoderm demonstrates uncoupling of somite compartmentalization and boundary formation. *Genes Dev* **22:** 2166–2171.

Fortini ME. 2009. Notch signaling: the core pathway and its posttranslational regulation. *Dev Cell* **16:** 633–647.

Harima Y, Takashima Y, Ueda Y, Ohtsuka T, Kageyama R. 2013. Accelerating the tempo of the segmentation clock by reducing the number of introns in the *Hes7* gene. *Cell Rep* **3:** 1–7.

Hirata H, Yoshiura S, Ohtsuka T, Bessho Y, Harada T, Yoshikawa K, Kageyama R. 2002. Oscillatory expression of the bHLH factor Hes1 regulated by a negative feedback loop. *Science* **298:** 840–843.

Hrabe de Angelis M, McIntyre II J, Gossler A. 1997. Maintenance of somite borders in mice requires the Delta homologue Dll1. *Nature* **386:** 717–721.

Imayoshi I, Kageyama R. 2014. bHLH factors in self-renewal, multipotency, and fate choice of neural progenitor cells. *Neuron* **82:** 9–23.

Imayoshi I, Isomura A, Harima Y, Kawaguchi K, Kori H, Miyachi H, Fujiwara TK, Ishidate F, Kageyama R. 2013. Oscillatory control of factors determining multipotency and fate in mouse neural progenitors. *Science* **342:** 1203–1208.

Isomura A, Kageyama R. 2014. Ultradian oscillators: rhythms and cell fate decisions. *Development* **141:** 3627–3636.

Jarriault S, Brou C, Logeat F, Schroeter EH, Kopan R, Israel A. 1995. Signalling downstream of activated mammalian Notch. *Nature* **377:** 355–358.

Jouve C, Palmeirim I, Henrique D, Beckers J, Gossler A, Ish-Horowicz D, Pourquié O. 2000. Notch signalling is required for cyclic expression of the hairy-like gene *HES1* in the presomitic mesoderm. *Development* **127:** 1421–1429.

Kageyama R, Ohtsuka T, Shimojo H, Imayoshi I. 2008. Dynamic Notch signaling in neural progenitor cells and a revised view of lateral inhibition. *Nat Neurosci* **11:** 1247–1251.

Kato TM, Kawaguchi A, Kosodo Y, Niwa H, Matsuzaki F. 2010. *Lunatic fringe* potentiates Notch signaling in the developing brain. *Mol Cell Neurosci* **45:** 12–25.

Kawaguchi D, Yoshimatsu T, Hozumi K, Gotoh Y. 2008. Selection of differentiating cells by different levels of delta-like 1 among neural precursor cells in the developing mouse telencephalon. *Development* **135:** 3849–3858.

Kobayashi T, Mizuno H, Imayoshi I, Furusawa C, Shirahige K, Kageyama R. 2009. The cyclic gene Hes1 contributes to diverse differentiation responses of embryonic stem cells. *Genes Dev* **23:** 1870–1875.

Kopan R, Ilagan MXG. 2009. The canonical Notch signaling pathway: unfolding the activation mechanism. *Cell* **137:** 216–233.

Levine JH, Lin Y, Elowitz MB. 2013. Functional roles of pulsing in genetic circuits. *Science* **342:** 1193–1200.

Lewis J. 2003. Autoinhibition with transcriptional delay: a simple mechanism for the zebrafish somitogenesis oscillator. *Curr Biol* **13:** 1398–1408.

Mara A, Schroeder J, Chalouni C, Holley SA. 2007. Priming, initiation and synchronization of the segmentation clock by *deltaD* and *deltaC*. *Nat Cell Biol* **9:** 523–530.

Maruhashi M, Van de Putte T, Huylebroeck D, Kondoh H, Higashi Y. 2005. Involvement of SIP1 in positioning of somite boundaries in the mouse embryo. *Dev Dyn* **234:** 332–338.

Masamizu Y, Ohtsuka T, Takashima Y, Nagahara H, Takenaka Y, Yoshikawa K, Okamura H, Kageyama R. 2006. Real-time imaging of the somite segmentation clock: revelation of unstable oscillators in the individual presomitic mesoderm cells. *Proc Natl Acad Sci* **103:** 1313–1318.

Niwa Y, Shimojo H, Isomura A, González A, Miyachi H, Kageyama R. 2011. Different types of oscillations in Notch and Fgf signaling regulate the spatiotemporal periodicity of somitogenesis. *Genes Dev* **25:** 1115–1120.

Oates AC, Morelli LG, Ares S. 2012. Patterning embryos with oscillations: structure, function and dynamics of the vertebrate segmentation clock. *Development* **139:** 625–639.

Okubo Y, Sugawara T, Abe-Koduka N, Kanno J, Kimura A, Saga Y. 2012. Lfng regulates the synchronized oscillation of the mouse segmentation clock via *trans*-repression of Notch signalling. *Nat Commun* **3:** 1141.

Ong CT, Cheng HT, Chang LW, Ohtsuka T, Kageyama R, Stormo GD, Kopan R. 2006. Target selectivity of vertebrate notch proteins. Collaboration between discrete domains and CSL-binding site architecture determines activation probability. *J Biol Chem* **281:** 5106–5119.

Panin VM, Shao L, Lei L, Moloney DJ, Irvine KD, Haltiwanger RS. 2002. Notch ligands are substrates for protein *O*-fucosyltransferase-1 and Fringe. *J Biol Chem* **277:** 29945–29952.

Parks AL, Klueg KM, Stout JR, Muskavitch MAT. 2000. Ligand endocytosis drives receptor dissociation and activation in the Notch pathway. *Development* **127:** 1373–1385.

Pierfelice T, Alberi L, Gaiano N. 2011. Notch in the vertebrate nervous system: an old dog with new tricks. *Neuron* **69:** 840–855.

Pourquié O. 2011. Vertebrate segmentation: from cyclic gene networks to scoliosis. *Cell* **145:** 650–663.

Purvis JE, Lahav G. 2013. Encoding and decoding cellular information through signaling dynamics. *Cell* **152:** 945–956.

Ramana Reddy DV, Sen A, Johnston GL. 1998. Experimental evidence of time delay induced death in coupled limit cycle oscillators. *Phys Rev Lett* **80:** 5109–5112.

Schuster-Gossler K, Cordes R, Gossler A. 2007. Premature myogenic differentiation and depletion of progenitor cells cause severe muscle hypotrophy in *Delta1* mutants. *Proc Natl Acad Sci* **104:** 537–542.

Shimojo H, Ohtsuka T, Kageyama R. 2008. Oscillations in notch signaling regulate maintenance of neural progenitors. *Neuron* **58:** 52–64.

Soza-Ried C, Öztürk E, Ish-Horowicz D, Lewis J. 2014. Pulses of Notch activation synchronize oscillating somite cells and entrain the zebrafish segmentation clock. *Development* **141:** 1780–1788.

Sparrow DB, Chapman G, Smith AJ, Mattar MZ, Major JA, O'Reilly VC, Saga Y, Zackai EH, Dormans JP, Alman BA, et al. 2012. A mechanism for gene-environment interaction in the etiology of congenital scoliosis. *Cell* **149:** 295–306.

Swinburne IA, Silver PA. 2008. Intron delays and transcriptional timing during development. *Dev Cell* **14:** 324–330.

Swinburne IA, Miguez DG, Landgraf D, Silver PA. 2008. Intron length increases oscillatory periods of gene expression in animal cells. *Genes Dev* **22:** 2342–2346.

Takashima Y, Ohtsuka T, González A, Miyachi H, Kageyama R. 2011. Intronic delay is essential for oscillatory expression in the segmentation clock. *Proc Natl Acad Sci* **108:** 3300–3305.

Wang X, Chen X, Yang Y. 2012. Spatiotemporal control of gene expression by a light-switchable transgene system. *Nat Methods* **9:** 266–269.

Yamamoto S, Charng W-L, Bellen HJ. 2010. Endocytosis and intracellular trafficking of Notch and its ligands. *Curr Top Dev Biol* **92:** 165–200.

Yun K, Fischman S, Johnson J, Hrabe de Angelis M, Weinmaster G, Rubenstein JLR. 2002. Modulation of the notch signaling by *Mash1* and *Dlx1/2* regulates sequential specification and differentiation of progenitor cell types in the subcortical telencephalon. *Development* **129:** 5029–5040.

Zhang N, Gridley T. 1998. Defects in somite formation in lunatic fringe-deficient mice. *Nature* **394:** 374–377.

Oscillatory control of Delta-like1 in cell interactions regulates dynamic gene expression and tissue morphogenesis

Hiromi Shimojo, Akihiro Isomura, Toshiyuki Ohtsuka, et al.

Genes Dev. 2016 30: 102-116
Access the most recent version at doi:10.1101/gad.270785.115